The Journal of Immunology

# Membrane-Type 6 Matrix Metalloproteinase Regulates the Activation-Induced Downmodulation of CD16 in Human Primary NK Cells



Giovanna Peruzzi, Laurette Femnou, Aleksandra Gil-Krzewska, Francisco Borrego, Jennifer Weck, Konrad Krzewski and John E. Coligan

*J Immunol* 2013; 191:1883-1894; Prepublished online 12 July 2013;
doi: 10.4049/jimmunol.1300313
http://www.jimmunol.org/content/191/4/1883



*The Journal of Immunology* is published twice each month by
The American Association of Immunologists, Inc.,
1451 Rockville Pike, Suite 650, Rockville, MD 20852

Print ISSN: 0022-1767 Online ISSN: 1550-6606.

# Membrane-Type 6 Matrix Metalloproteinase Regulates the Activation-Induced Downmodulation of CD16 in Human Primary NK Cells

**Giovanna Peruzzi,*,[1] Laurette Femnou,* Aleksandra Gil-Krzewska,* Francisco Borrego,[†] Jennifer Weck,* Konrad Krzewski,*,[2] and John E. Coligan*,[2]**

**CD16 (FcγRIIIa), the low-affinity receptor for IgG, expressed by the majority of human NK cells, is a potent activating receptor that facilitates Ab-dependent cell-mediated cytotoxicity (ADCC). ADCC dysfunction has been linked to cancer progression and poor prognosis for chronic infections, such as HIV; thus, understanding how CD16 expression is regulated by NK cells has clinical relevance. Importantly, CD16 cell-surface expression is downmodulated following NK cell activation and, in particular, exposure to stimulatory cytokines (IL-2 or IL-15), likely owing to the action of matrix metalloproteinases (MMPs). In this article, we identify membrane-type 6 (MT6) MMP (also known as MMP25) as a proteinase responsible for CD16 downmodulation. IL-2–induced upregulation of MT6/MMP25 cell-surface expression correlates with CD16 downmodulation. MT6/MMP25, sequestered in intracellular compartments in unstimulated NK cells, translocates to the cell surface after stimulation; moreover, it polarizes to the effector–target cell interface of the CD16-mediated immunological synapse. siRNA-mediated disruption of MT6/MMP25 expression enhances the ADCC capacity of NK cells, emphasizing the important functional role of MT6/MMP25 in the regulation of ADCC activity. Thus, this study uncovers a previously unknown role of MT6/MMP25 in human NK cells, and suggests that inhibition of MT6/MMP25 activity could improve ADCC efficacy of therapeutically administered NK cells that require IL-2 for culture and expansion.** ***The Journal of Immunology*****, 2013, 191: 1883–1894.**

Natural killer cells constitute a subset of lymphocytes that play a pivotal role in the first-line defense against pathogen-infected, tumorigenic, and otherwise stressed cells (1). NK cells express a large number of germline-encoded activating receptors that recognize ligands expressed by such abnormal cells, which trigger NK cell inflammatory cytokine secretion and/or target cell cytolysis. Because, in some circumstances, activating receptors have the potential to recognize normal cells, NK cells also express a panel of inhibitory receptors that thwart unwanted self-reactions (2). In addition, to dampen stimulatory signals and thus control for excessive inflammation, which can be dangerous to the host, activating receptors are often downmodulated by endocytosis and routed to lysosomes for degradation (3–6). Moreover, activating receptors, as, for example, CD16, can be also downmodulated by proteolytic cleavage (7, 8).

CD16 (FcγRIIIa) binds to the Fc portion of IgG1 and IgG3, is expressed by the majority of human NK cells, and is a potent activating receptor that mediates Ab-dependent cell-mediated cytotoxicity (ADCC) (9). As the IgG–CD16 interaction is of low affinity, the bound IgG can be readily exchanged, thereby greatly expanding the repertoire of target cells that can be recognized by NK cells. ADCC activity has been associated with better outcomes for some type of cancers (10), chronic viral infections (11), and autoimmune diseases (12). Furthermore, many therapeutic mAbs that specifically recognize tumor cells are able to bind to CD16 on NK cells, promoting NK cell–mediated ADCC of these tumor cells (13–17). Not surprisingly, downmodulation of CD16 expression by NK cells, leading to the impairment of NK cell–mediated ADCC, has been linked to increased disease severity in, for instance, chronic infections such as HIV (18). Thus, identification of the mechanism(s) responsible for CD16 downmodulation has clinical significance.

The potency of NK cell–mediated cytotoxicity toward malignant cells via CD16, coupled with the ability to produce therapeutic Abs specific for tumor cell-surface Ags, has propelled efforts to expand patients' NK cells in vitro for immunotherapeutic reinfusion. The expansion of primary NK cells in vitro requires cytokines of the common γ-chain (γc) family, usually IL-2 (19, 20). A potential detrimental effect of this IL-2–induced expansion is that IL-2 is known to upregulate expression of the matrix metalloproteinases (MMPs) in primary NK cells (21). Members of the MMP family are zinc-dependent endopeptidases that were initially characterized as being responsible for extracellular matrix degradation, although other substrates are now recognized (22–24). Membrane-type (MT) MMPs contain either GPI anchors or transmembrane domains. MMPs have been shown to modulate NK cell cytotoxicity by cleaving activating receptors from the cell surface of human primary NK cells (7, 8), including CD16 (25). This finding agrees with a report demonstrating that in HIV-

*Receptor Cell Biology Section, Laboratory of Immunogenetics, National Institute of Allergy and Infectious Diseases, National Institutes of Health, Rockville, MD 20852; and [†]BioCruces Health Research Institute, Ikerbasque, Basque Foundation for Science, 48903 Bizkaia, Spain

[1]Current address: Department of Molecular Medicine, "Sapienza" Università di Roma, Rome, Italy.

[2]K.K. and J.E.C. contributed equally to this work.

Received for publication January 31, 2013. Accepted for publication June 17, 2013.

G.P., L.F., J.W., and A.G.-K. performed the experiments; G.P., L.F., A.G.-K., F.B., J. W., K.K., and J.E.C. analyzed the results; G.P., F.B., J.W., K.K., and J.E.C. designed the research; and G.P., J.W., K.K., and J.E.C. wrote the paper.

Address correspondence and reprint requests to Dr. John E. Coligan, National Institute of Allergy and Infectious Diseases, National Institutes of Health, Twinbrook II, Room 205, 12441 Parklawn Drive, Rockville, MD 20852. E-mail address: jcoligan@niaid.nih.gov

The online version of this article contains supplemental material.

Abbreviations used in this article: ADCC, Ab-dependent cell-mediated cytotoxicity; MFI, median fluorescence intensity; MMP, matrix metalloproteinase; MT, membrane-type; MT6/MMP25, MT6-MMP, also known as MMP25; PAO, phenylarsine oxide; siRNA, small interfering RNA; TIMP, tissue inhibitor of metalloproteinase.

www.jimmunol.org/cgi/doi/10.4049/jimmunol.1300313

infected patients, impaired NK cell ADCC correlated with decreased CD16 cell-surface levels, and inversely correlated with an increase in MMP transcript levels (18). Treatment of these cells with a general MMP inhibitor partially restored both CD16 expression and the ability of NK cells to recognize and kill target cells by ADCC. Several other reports suggest that progressive HIV infection is associated with a high production of MMPs, as reviewed in Ref. 26. Thus, MMPs appear to play a very important role in regulating CD16 expression.

In this article, we show that the activating cytokine IL-2 not only increases transcript levels of MT6-MMP (also known as MMP25, and herein referred to as MT6/MMP25) but also induces the translocation of MT6/MMP25 protein from intracellular compartments, where it is localized in unstimulated NK cells, to the cell surface. This activity correlates with the downregulation of CD16 expression from the surface of human primary NK cells. During ADCC-mediated target cell engagement, MT6/MMP25 polarizes to the immunological synapse, which agrees with the finding that reducing MT6/MMP25 expression via siRNA enhances ADCC.

## Materials and Methods

### *Chemical reagents and Abs*

Anti-CD3 APC-conjugated mAb (clone UCHT1), anti-CD56 PE-conjugated mAb clone CMSSB, and anti-human CD16 mAb (clone CB16) were from eBioscience. Anti-human NKG2D PE-conjugated mAb (clone 149810), anti-human MT6/MMP25 mAb (clone 141811), and anti-human MT1/MMP14 mAb (clone 128527) were from R&D Systems. Anti-perforin Alexa Fluor 647–conjugated (clone δG9) was from BioLegend. Dylight 488– or 549–conjugated goat anti-mouse IgG, Fcγ1 or Fcγ2b specific, was from Jackson ImmunoResearch Laboratories. Alexa Fluor 647–conjugated goat anti-mouse IgG1 and FITC-conjugated goat anti-mouse IgG were from Invitrogen; anti-CD16–PE (clone 3G8), anti-CD28–PE (clone CD28.2), and anti-CD71 (clone YDJ.1.2.2) mAbs were from Beckman Coulter. Herceptin (trastuzumab), an anti-HER2 humanized mAb, was kindly provided by Drs. Wen Jin Wu and Milos Dokmanovic (Food and Drug Administration, Bethesda MD). Human CD16, cloned into the lentiviral vector pCDH encoding a puromycin resistance gene, was kindly provided by Dr. Eric Long (National Institute of Allergy and Infectious Diseases, National Institutes of Health, Rockville MD). The MMP inhibitor GM6001 was from Calbiochem. All other chemicals and reagents were obtained from Sigma-Aldrich unless otherwise mentioned.

### *Cell culture*

Primary NK cells were isolated from human peripheral blood using EasySep NK Cell isolation kits (Stem Cell Technology), and their purity (>95%) was determined by flow cytometry analysis following staining with anti-CD3 and anti-CD56 mAbs. NK cells were cultured in X-VIVO Medium (Lonza) containing 10% human AB serum (Valley Biomedical) and rIL-2 (500 U/ml) (National Cancer Institute , Frederick, MD), unless otherwise stated. In some experiments, IL-15 was used (10 ng/ml; PeproTech;). The human NK tumor cell line YTS, the B lymphoblastoid cell line 721.221, and the human ovarian carcinoma cell line SK-OV3 were grown in complete RPMI 1640 medium (Invitrogen). NKL cells were cultured in complete RPMI 1640 medium with 100 U/ml IL-2. The YTS cells transduced with pCDH-CD16 were grown in complete RPMI 1640 medium supplemented with puromycin (0.5 μg/ml).

### *RT-PCR and real time PCR*

RNA was isolated with RNAqueous-4PCR kits (Ambion) with the DNAse treatment step, and cDNA was generated using Qscript (Quanta BioSciences). Primers used for amplifying human MMPs were purchased from QIAGEN. PCR reactions were performed using standard protocols. Real-time PCR was performed on a Roche LightCycler 480 using LightCycler 480 SYBR Green I Master Mix (Roche Diagnostics). All reactions were performed in triplicate, and averages were used to calculate the levels of each mRNA, based on standard curves generated from pooled cDNA. Relative quantification of the target genes was determined using the second derivative maximum with Roche LightCycler software, and normalizing each transcript level to that of 18S rRNA. Fold changes were calculated by setting the normalized transcript level of unstimulated samples to one. Melting curve analyses were performed at the end of each run to ensure that only one product was amplified.

### *Lentiviral vector transduction*

The pCDH-CD16 lentiviral expression construct was transfected into 293T cells with the psPAX2 and pMD2.G helper plasmids (Addgene) using FuGENE 6 HD (Roche). The medium containing lentivirus particles was added to $2 \times 10^6$ YTS cells, and the infection was carried out for 12 h in the presence of 8 μg/ml protamine sulfate. After 48 h, YTS cells were transferred to medium containing puromycin (0.5 μg/ml) and maintained in the selection medium to generate a stable YTS cell line overexpressing CD16.

### *Flow cytometry*

CD16, CD28, and NKG2D cell-surface expression levels were assessed by staining with PE-conjugated mAb for 30 min on ice, followed by washing with PBS containing 0.05% FBS. For detection of MT6/MMP25 and MT1/MMP14, cells were stained with unlabeled primary Abs for 30 min on ice and, after extensive washing, incubated with FITC-conjugated goat anti-mouse IgG. In all experiments, isotype control Abs were used to monitor background staining levels. For analysis of total protein levels, cells were fixed, permeabilized with Cytofix/Cytoperm Buffer (BD Biosciences), and processed as above. For CD16 and MT6/MMP25 double staining experiments, cells were incubated with anti-MT6/MMP25 Ab, as mentioned above, followed by blocking with 5% mouse serum and staining with PE-conjugated anti-CD16 Ab. For all experiments, the data were acquired using the FACSort cytometer (BD), and analyses were performed using FlowJo software (v. 7.6; TreeStar).

### *Activation of NK cells with PMA, MMP inhibition, and receptor cell-surface level assessment*

Freshly isolated NK cells, or NK cells cultured for 2 d in the presence of IL-2 (500 U/ml) in X-VIVO Medium without human serum, were incubated with PMA (200 ng/ml) or vehicle alone (DMSO). For MMP inhibition studies, cells were treated either with PMA plus GM6001 (10 μM), with PMA plus 1,10-phenanthroline monohydrate (2 mM), or with IL-2 (500 U/ml) plus GM6001 (10 μM) for the indicated times. 1,10-Phenanthroline monohydrate inhibits MMPs by binding metals in metalloenzymes, and GM6001 is a potent broad-spectrum inhibitor of MMPs. In experiments evaluating CD16 release from the surface of activated cells, NK cells were preincubated with PE-conjugated anti-CD16 mAb for 30 min on ice, followed by treatment with PMA or PMA plus GM6001 for 3 h at 37˚C. Cells treated with GM6001 were preincubated with the inhibitor 1 h prior to PMA addition. In the experiments using phenylarsine oxide [(PAO), 5 μM] or dynasore (80 μM), the inhibitors were added at time 0. An aliquot of cells was collected every 30 min, and the CD16 surface expression levels were determined by flow cytometry.

Endocytosis of CD71 in the NK cell line, NKL, was used as a control to determine the drug efficacy. NKL cells were incubated with 5 μg anti-CD71 mAb for 30 min on ice. The cells were washed twice and then kept at 37˚C for the indicated times to allow receptor internalization. The cells were then stained with FITC-conjugated goat anti-mouse Ab on ice to label the remaining CD71 on the cell surface, and analyzed by flow cytometry. In the experiment using PAO, cells were pretreated with the drug (5 μM) at 37˚C for 30 min. The inhibitor concentration was maintained during the internalization process. The percentage of endocytosis was calculated as the difference between the median fluorescence intensity (MFI) value of the receptor cell-surface staining at time 0 (taken as 100%) and at 60 min, i.e., percentage endocytosis = $100 - [(\text{MFI 60 min}/\text{MFI time 0}) \times 100]$.

### *Detection of released CD16*

The determination of released CD16 from PMA-activated cells was done using the Synergy 2 Multi-Mode Microplate Reader (BioTek), according to the manufacturer's instructions. Human primary NK cells were incubated on ice with PE-conjugated anti-CD16 mAb (clone 3G8) for 30 min. Next, cells were resuspended in PBS and left untreated (control) or were treated with PMA orwith PMA plus GM6001 at 37˚C for 3 h. Cell supernatants were collected, and PE fluorescence was measured to evaluate the receptor release. Supernatants from unlabeled cells were used as blanks (background), and the fluorescence of cells stained with anti-CD16 PE was used to estimate the total level of CD16 on the cell surface. The amount of released CD16 was calculated according to the following formula: (sample release fluorescence − background)/(total CD16 level − background). The fold change was determined by comparison with the control (supernatant of the untreated cells). Each sample was done in triplicate.

### *Measurement of cytotoxicity*

The cytotoxicity of YTS/pCDH-CD16 cells was evaluated by lanthanide (Europium) fluorescence assay using DELFIA cytotoxicity reagents (Per-

kinElmer), according to the manufacturer's instructions. Briefly, target cells were labeled with BATDA for 30 min at 37°C in complete RPMI 1640 medium. Labeled cells were transferred to 96-well polystyrene plates (U-bottom, NUNC), mixed with YTS at the indicated E:T ratios, and incubated for 2 h at 37°C. For ADCC, SK-OV3 target cells labeled with BATDA reagent, were incubated with 50 ng/ml of either anti-HER2 mAb or control human IgG1 (EMD Chemicals, Calbiochem), spun down, resuspended in medium, and plated at $10^4$ cells per well in triplicate. NK or YTS/pCDH-CD16 cells were added to wells at the indicated E:T ratios. After 2 h incubation, the supernatant was collected, and the release of TDA was measured according to the manufacturer's instructions, using a Wallac VICTOR2 plate reader (PerkinElmer). The amount of released TDA in cell supernatants was regarded as the experimental TDA release. Total TDA release was measured after complete lysis of target cells by 1% Triton X-100. Lysis percentage was calculated using the following equation: (experimental TDA release − spontaneously released TDA)/(total TDA release − spontaneously released TDA) × 100.

### *Confocal microscopy and image analysis*

To visualize the CD16-mediated immune synapses between NK and SK-OV3 cells, $2 \times 10^5$ NK cells were mixed with $4 \times 10^5$SK-OV3 target cells, and incubated for 20 min at 37°C in X-VIVO Medium, in the presence of 50 ng/ml of either anti-Her2 mAb or control human IgG1, followed by adherence to Excell Adhesion slides (Electron Microscopy Sciences) for 20 min at 37°C. Cells were fixed, permeabilized using Cytofix/Cytoperm Buffer with 0.1% Triton X-100, and blocked with 1% BSA. The cells were then stained with anti-MT6/MMP25 mAb, followed by IgG1-specific DyLight 488– or 549–conjugated anti-mouse Ab, or Alexa Fluor 647–conjugated goat and mouse IgG1 (as specified for each experiment in figure legends), blocked with 5% normal mouse serum, and then stained with Alexa Fluor 488– or 647–conjugated anti-perforin (δG9). For triple staining of perforin, MT1/MMP14, and MT6/MMP25, the permeabilized cells were stained in the following order, to avoid cross-reactivity between Abs to perforin and MT1/MMP14 that share the same isotype (IgG2b): MT1/MMP14, MT6/MMP25 (both primary and secondary Abs), and directly conjugated perforin with a blocking step (5% normal mouse serum) between incubations. In experiments involving visualization of CD16, human primary NK cells were fixed, permeabilized, and stained with unlabeled anti-CD16 mAb, followed by IgG1-specific DyLight 488–conjugated anti-mouse Ab. To visualize MT6/MMP25 recruitment at the contact site, protein G polystyrene beads (6.8 μm) were precoated with anti-CD16 mAb for 60 min at 4°C, mixed with YTS/pCDH-CD16 cells and incubated 45 min at 37°C, then transferred to slides, fixed, and stained with anti-MT6/MMP25 mAb, followed by IgG1-specific DyLight 488–conjugated anti-mouse Ab. For each experiment, cells mounted in ProLong Gold medium were visualized using a Zeiss LSM 510 Axiovert 200M laser-scanning confocal microscope at room temperature. The images were acquired using ×63 Zeiss Plan-APOCHROMAT objective (Carl Zeiss). Images shown represent a single optical section.

### *Small interfering RNA transfection*

YTS cells stably transduced with CD16 were nucleofected with 4 μM small interfering RNA (siRNA) duplexes, using Nucleofector Kit R, according to the manufacturer's instructions (Lonza). To achieve knockdown of human MT6, five oligos were tested for their silencing efficiency in the NK cell lines (data not shown), and the two most efficient oligomers (5′-CAGCUUGACUCCCAUCAAC-3′ and 5′-CUCAACGCUGGUGGAAAGA-3′) were used in subsequent experiments, in parallel with an siRNA universal negative control (Sigma-Aldrich). The cell viability after siRNA transfections was 60–70%. The silencing efficiency was evaluated by the measurement of average fluorescence intensity values of anti-MT6/MMP25 staining per cell, using confocal microscopy and ImageJ.

### *Statistical analysis*

For all experiments, statistical analysis and graphing were done using the Graphpad Prism 5 software. Two-tailed, unpaired or paired Student *t* test, or one-way ANOVA (as indicated in figure legends) was used to compare the statistical significance of the differences observed between samples. Asterisks indicate statistical significance: $*p < 0.05$, $**p < 0.005$, $***p < 0.001$.

## Results

### *CD16 cell-surface expression is downmodulated by IL-2 in human primary NK cells*

IL-2 or IL-15 is necessary for the proliferation and survival of NK cells in culture (20); however, human NK cells cultured and expanded in the presence of IL-2 markedly reduced CD16 cell-surface expression (Fig. 1A). The downmodulation of cell-surface CD16 was likely an active posttranslational process, as CD16 mRNA was stable during the first 3 d of culture, and even started to increase after 4 d (Fig. 1B). The downmodulation of CD16 could be detected as early as 6 h post IL-2 treatment (Fig. 1C, *second histogram in each row*). As with IL-2, culturing of NK cells with IL-15 also led to downmodulation of CD16 from the surface of NK cells (Fig. 1C, *third histogram in each row*). On average, 6 h of culture with IL-2 or IL-15 led to ∼ 10% downmodulation of CD16, whereas after 12 and 24 h, the levels of CD16 decreased by ∼ 25% and ∼ 50%, respectively (Fig. 1C, *bottom graph*). This time was too short to allow for expansion of the small fraction of $CD56^{bright}CD16^{dim/-}$ NK cells that express the high-affinity receptor for IL-2 (CD25, IL-2Rα) (27), as essentially no proliferation of NK cells occurred during the first 48 h of culture with IL-2 (Supplemental Fig.1); thus, the observed loss of CD16 was not due to increased proliferation of $CD16^-$ cells. Importantly, the removal of IL-2 from cultured NK cells restored CD16 expression, providing confirmation that IL-2 induced CD16 downmodulation (Fig. 1D). Finally, to further substantiate that IL-2 leads to CD16 downmodulation, we examined its effect on CD16 expression by the YTS NK cell line that grows independently of IL-2. We found that, as with primary NK cells, CD16 expression was downmodulated when YTS cells were cultured with IL-2 (Fig. 1E, *upper panel*). In contrast, the expression of another cell-surface activating receptor, CD28, was not affected by culture with IL-2 (Fig. 1E, *lower panel*). In toto, these data indicate that the activating cytokine IL-2 is involved in CD16 downmodulation.

### *The activation-induced loss of CD16 in human primary NK cells is restored by MMP inhibition*

Because IL-2 induced the downmodulation of CD16 expression on the cell surface of cultured NK cells, and has been shown to upregulate several metalloproteinases (21), we examined whether the treatment of NK cells with an MMP inhibitor would affect the IL-2–mediated decrease of CD16 levels. Therefore, we cultured the freshly isolated human NK cells for 24 h either in the absence of IL-2 or in the presence of IL-2 with or without an MMP inhibitor (GM6001). We found that although the addition of IL-2 alone induced almost 60% downmodulation of CD16 from the cell surface, the addition of MMP inhibitor partially rescued the CD16 cell-surface levels (Fig. 2A), indicating that IL-2–induced MMP activity could be responsible for the decrease of CD16 on the surface of stimulated NK cells.

NK cell activation through the IL-2R pathway leads to the Ras/MAPK signaling cascade (28). The phorbol ester PMA, commonly used to stimulate lymphocytes, directly activates protein kinase C in this signaling cascade and serves as a generalized means of activating NK cells. NK cells treated with PMA rapidly downmodulated 95% of CD16 from the cell surface (Fig. 2B, *upper panels*) (29). This downmodulation was not a general effect, as another important NK activating receptor, NKG2D, was not affected by PMA treatment (Fig. 2B, *lower panels*). As with IL-2, the CD16 downmodulation was markedly inhibited (∼50%) by the presence of the MMP inhibitors GM6001 or 1,10 phenanthroline (Fig. 2B, *upper panels*), indicating that proteolytic cleavage is involved in CD16 downmodulation. To verify that shedding and not endocytosis was responsible for CD16 downmodulation, human primary NK cells were incubated with PE-labeled anti-CD16 mAb on ice and subsequently treated with PMA, or PMA plus GM6001, in the presence or absence of an endocytic pathway inhibitor, PAO (30). We observed a time-dependent CD16 downmodulation from the cell surface that was not affected by the

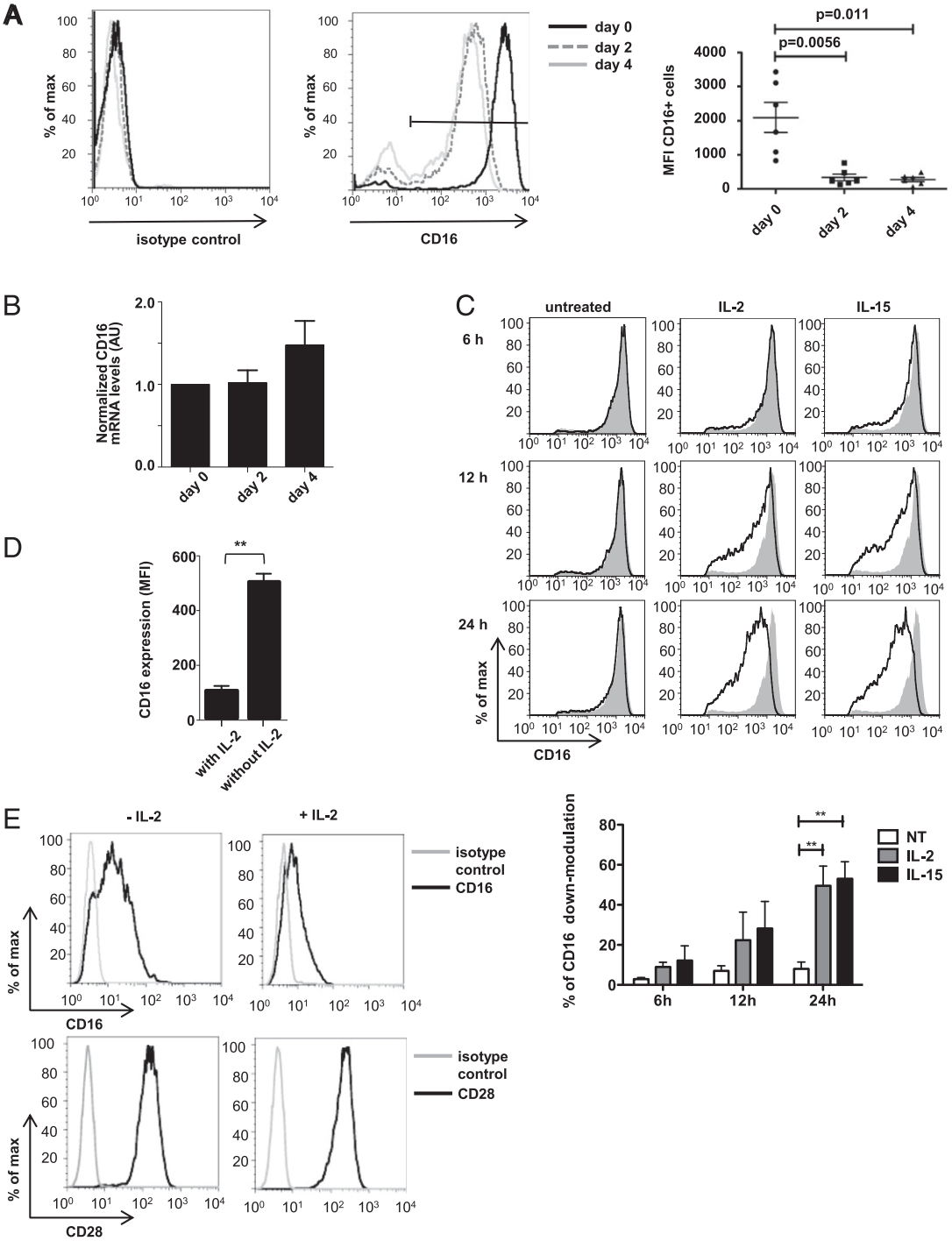


**FIGURE 1.** CD16 cell-surface expression is downmodulated by IL-2 in human NK cells. (**A**) Freshly isolated human NK cells were cultured in X-VIVO Medium in the absence of human serum and in the presence of IL-2 (500 U/ml). CD16 cell-surface expression was evaluated by flow cytometry at day 0 (freshly isolated cells) and after 2 or 4 d of culture. The *histogram on the right* shows the CD16 staining, and the *histogram on the left* shows the isotype control staining for an individual donor. The range gate shown in the histogram was used for the evaluation of $CD16^+$ cells. The graph on the *right* shows MFI of $CD16^+$ cells from six independent analyses with different donors. Error bars indicate SEM. Statistical analysis was performed using the two-tailed paired Student *t* test. The *p* values are indicated in the figure. (**B**) CD16 transcript levels from NK cells cultured for 0, 2, or 4 d were determined by quantitative RT-PCR. Results shown are normalized to 18S rRNA. The graph summarizes data obtained from six independent donors [same as in (A)]. (**C**) Freshly isolated human NK cells were cultured without (*first column*) or with IL-2 (500 U/ml) (*second column*), or IL-15 (10 ng/ml) (*third column*), for the indicated times. The analyzed cells were gated on the $CD56^{dim}$ subset. In each panel, a gray-filled histogram represents time 0, and the black line histogram represents CD16 expression level with culture in IL-2, IL-15, or without cytokines. The bar graph at the bottom summarizes data from four independent experiments with different donors; error bars indicate SEM. Statistical analysis was done using the two-tailed paired Student *t* test. (**D**) IL-2–cultured human NK cells were analyzed for CD16 surface expression under normal culture conditions (with IL-2), and 24 h after IL-2 removal (without IL-2). The graph shows the MFI values for CD16 expression and summarizes the values obtained from four independent donors + SEM. Statistical analysis was done using the two-tailed paired Student *t* test. (**E**) YTS cells were cultured for 4 d in the absence or presence of IL-2 (500 U/ml). Cells were then stained with anti-CD16 (*upper panels*) or anti-CD28 (*lower panels*) Abs and analyzed by flow cytometry to determine the cell-surface levels of the receptors. Gray histograms represent isotype control staining. The result shown is representative of five independent experiments. $^{**}p < 0.005$.

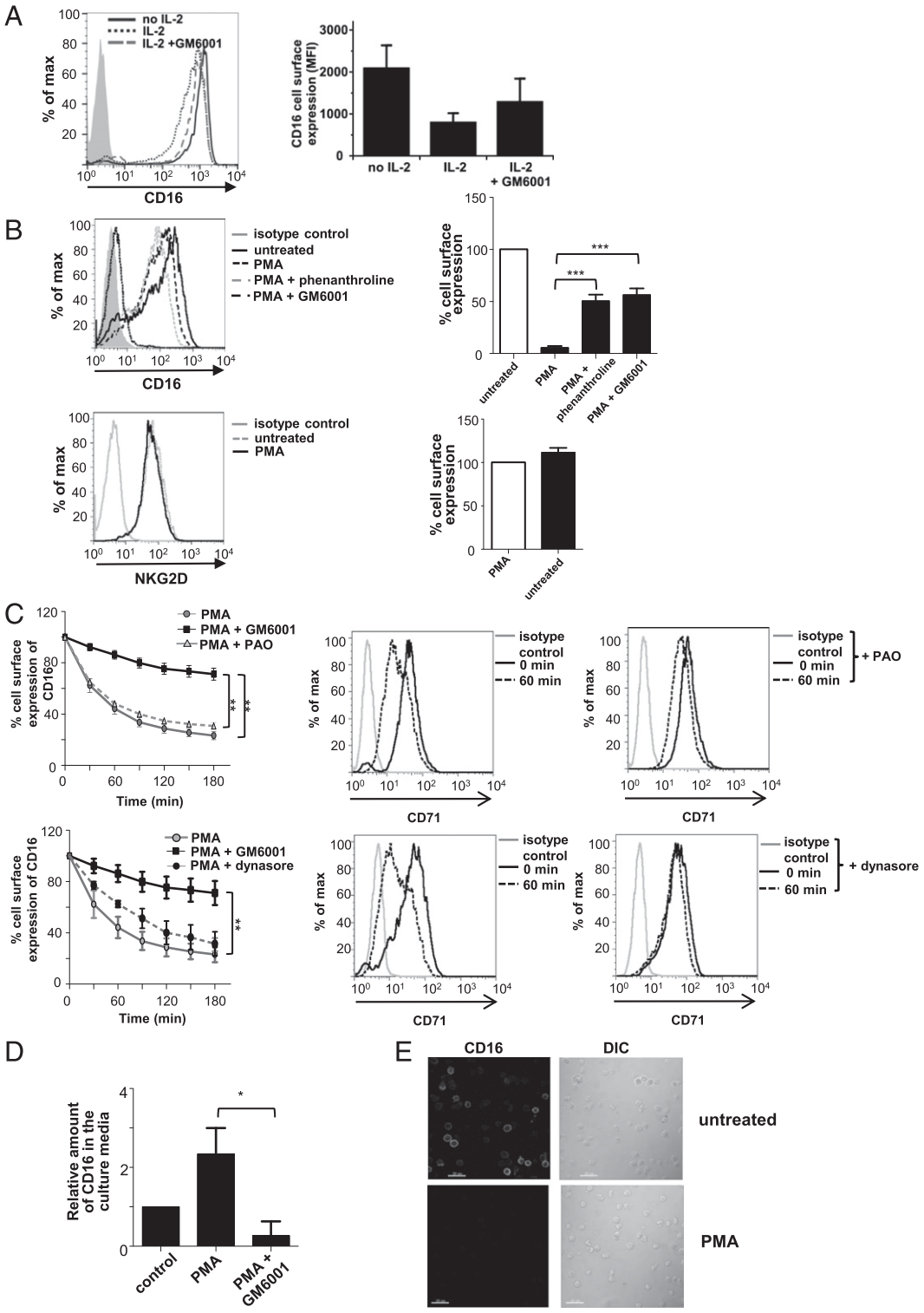


**FIGURE 2.** The activation-induced shedding of CD16 by human primary NK cells is restored by MMP inhibition. (**A**) Freshly isolated human NK cells were cultured in X-VIVO Medium without human serum for 24 h, either in the absence of IL-2 or in the presence of IL-2 (500 U/ml), or IL-2 and MMP inhibitor GM6001, and then analyzed by flow cytometry for CD16 expression. The *histogram on the left* shows an example of CD16 cell-surface expression for an individual donor; the gray-filled histogram represents isotype control staining, the solid line represents the level of CD16 on the cell surface of cells cultured without IL-2, the dotted line shows CD16 cell-surface expression after IL-2 treatment, and the dashed line illustrates the cell-surface expression of CD16 in cells treated with IL-2 and the MMP inhibitor. The *graph on the right* shows the MFI values of $CD16^+$ cells from three different donors. Error bars indicate SEM. (**B**) *Top panel*, Freshly isolated human primary NK cells were treated 3 h with DMSO solvent (untreated), PMA (200 ng/ml), or PMA plus MMP inhibitors, and then analyzed by flow cytometry for CD16 expression. The gray-filled histogram represents isotype control staining. The MMP inhibitors 1,10 phenanthroline and GM6001 were used at the concentration of 2 mM and 10 μM, respectively. The *right panel* shows the average from experiments with five different donors. *Bottom panel*, Freshly isolated human primary NK cells were treated for 3 h with DMSO (untreated) or PMA, then analyzed by flow cytometry for NKG2D expression. The gray line histogram represents isotype control staining. The *right panel* shows the average of experiments performed with four independent donors. The percentage of CD16 or NKG2D cell-surface expression by DMSO-treated cells (taken as 100%) is compared with PMA- and PMA plus phenanthroline- or GM6001-treated cells. Error bars indicate the SEM. Statistical (*Figure legend continues*)

presence of PAO, indicating that CD16 was not endocytosed but shed from the cell surface (Fig. 2C, *upper left panel*). To verify the efficacy of the drug, we confirmed that the endocytosis of CD71 (transferrin receptor) was significantly impaired by the presence of the drug (28% endocytosis with PAO compared with 60% without PAO) (Fig. 2C, *upper right and middle panels*). To further demonstrate that the PMA-induced CD16 downmodulation is not due to receptor endocytosis, we also used a specific dynamin inhibitor, dynasore (31). As with PAO, dynasore did not interfere with PMA-induced loss of CD16 from the cell surface (Fig. 2C, *lower left panel*) but blocked CD71 endocytosis (Fig. 2C, *lower right and middle panels*). Furthermore, we monitored the release of CD16 into the culture medium. We found that the cell culture media from PMA-treated cells contained significantly more (almost 8-fold) CD16 than media from the cells treated with PMA plus GM6001 (Fig. 2D). Finally, examination of NK cells by confocal microscopy confirmed that CD16 was not internalized. As shown in Fig. 2E, PMA-treated cells had no or little detectable intracellular CD16, confirming that CD16 is mainly shed by these cells, and not endocytosed. Therefore, we conclude that CD16 is cleaved in an MMP-dependent manner from the surface of activated NK cells.

### *IL-2 induces MT6/MMP25 expression and its translocation to the cell surface in human primary NK cells*

MMPs have been implicated in CD16 downmodulation by human primary NK cells (7), but information regarding which MMPs are expressed and function in cytotoxic lymphocytes is still limited (32). Because the MMP family of proteins is very large, we chose to concentrate our initial studies on those MMPs reported to be expressed in human NK cells and regulated by IL-2, namely, MMPs 2, 9, 13, 14 (MT1), 16 (MT3), and 25 (MT6) (21). As MT-MMPs are known to be involved in the shedding of receptors from other cell types, we also included the other MT-MMPs, 15 (MT2), 17 (MT4), and 24 (MT5), as well as MMP7, which has been shown to be expressed in rodent NK cells (33).

Endpoint RT-PCR using cDNA generated from human NK cells, either freshly isolated or cultured in the presence of IL-2 for 4 d, indicated that MMP2, MMP9, MT1/MMP14, MT6/MMP25, and possibly MMP7 were expressed, and that MMP2, MT1/MMP14, and MT6/MMP25 might be positively regulated by IL-2 (Fig. 3A, *left*). Real-time PCR revealed that MMP7, MT2/MMP15, MT4/MMP17, and MT5/MMP24 were not expressed in either freshly isolated or IL-2–cultured human NK cells (when compared with no transcript controls; data not shown). These transcripts were detectable using cDNA from NK cell lines, indicating that the primers were functional (data not shown). Although not detectable in real-time PCR, the endpoint PCR showed the presence of a faint band corresponding to MMP7 transcripts in NK cells. This was probably the result of a nonspecific amplification caused by the excessive number of cycles used for the endpoint PCR.

The real-time PCR analysis revealed that only MMP9, MT1/MMP14, and MT6/MMP25 were regulated by IL-2 (Fig. 3A). MMP2 appeared not to be regulated by IL-2, and MMP9 was downregulated by IL-2 (Fig. 3A, *last two graphs*), consistent with a previous report (21), whereas the transcripts for MT1/MMP14 and MT6/MMP25 were significantly increased (1.7- and 3.5-fold, respectively) in the presence of IL-2 (Fig. 3A, *first two graphs*). Because MT1/MMP14 and MT6/MMP25 transcripts were upregulated by IL-2, we decided to further investigate the protein expression of these metalloproteinases in human primary NK cells. Flow cytometric analysis demonstrated that MT1/MMP14 was expressed on the surface in freshly isolated cells (Fig. 3B; minus IL-2). MT1/MMP14 expression decreased upon IL-2 stimulation (day 4; Fig. 3B, *right side histograms*), indicating that MT1/MMP14 is likely released from such NK cells. Importantly, we found that freshly isolated NK cells did not express MT6/MMP25 on the cell surface, suggesting that MT6/MMP25 is redistributed from intracellular compartments to the cell surface upon IL-2 activation (Fig. 3B, *left side histograms*). The appearance of MT6/MMP25 on the cell surface in response to IL-2 stimulation correlated with the downmodulation of CD16 (Fig. 3B, *two bottom panels*). Moreover, double staining for MT6/MMP25 and CD16 showed that the pool of cells acquiring the proteinase at the cell surface upon IL-2 stimulation is the same pool of cells that have downregulated CD16 expression (Fig. 3C). Indeed, after 2 d of culture with IL-2, CD16 expression was markedly reduced among MT6/MMP25$^+$ cells (CD16 MFI = 64), when compared with the MT6/MMP25$^-$ cells (CD16 MFI = 313) (Fig. 3C, *right panels*). These data show that MT6/MMP25 relocates to the cell surface upon cytokine treatment, and that IL-2–activated NK cells consist of a pool of cells expressing MT6/MMP25 and low levels of CD16 on the cell surface.

### *MT6/MMP25 polarizes and accumulates at the contact area between NK cells and target cells*

Because engagement of CD16 itself is a potent way to downmodulate CD16 (25), we investigated whether MT6/MMP25 plays a role in regulating ADCC. To visualize MT6/MMP25 distribution in the CD16-mediated immunological synapse during ADCC, we used confocal microscopy to analyze NK cells that were mixed with the human ovarian carcinoma HER2$^+$ cell line, SK-OV3, in the presence of Herceptin, a humanized IgG1 Ab targeting HER2 protein (34). Once CD16 binds to the Fc region of Herceptin that is coating the HER2$^+$ SK-OV3 cell, the NK cell undergoes activation. Strikingly, in the absence of target cells, perforin and MT6/MMP25 were dispersed throughout the cell with a minimal overlap (Fig. 4A, *upper panel*), indicating that in resting NK cells the proteinase resides in compartments that are distinct from the lytic granules. Following cell activation, MT6/MMP25 polarizes to the cell–cell contact site, along with perforin (Fig. 4A, *lower*

analysis was performed using the two-tailed paired Student *t* test. ***$p < 0.001$. (**C**) Freshly isolated human primary NK cells were incubated on ice with PE-conjugated anti-CD16 mAb, then resuspended in PBS and treated with PMA, PMA plus GM6001, PMA plus PAO, or PMA plus dynasore. An aliquot was taken every 30 min, and the level of CD16 on the cell surface was evaluated by flow cytometry. The graphs represent the percentage of CD16 expression on the surface of PMA-, PMA plus GM6001–, PMA plus PAO–treated cells (*upper left panel*), and PMA plus GM6001– and PMA plus dynasore–treated cells (*lower left panel*) compared with time 0 (taken as 100%, and equivalent to the DMSO-treated cells). The results shown represent the average of four experiments with different donors; error bars represent SEM. The *middle and right panels* show flow cytometry data for the endocytosis of CD71 in the presence (*right*) or absence (*middle*) of PAO (*upper*) or dynasore (*lower*). **$p < 0.005$. (**D**) CD16 released from freshly isolated NK cells, following PMA or PMA plus GM6001 treatment (see *Materials and Methods* for the detailed protocol). Data shown are expressed as a fold change when compared with the control sample and illustrate the average of four independent experiments with different donors; error bars indicate SEM. Statistical analysis was done using the two-tailed paired Student *t* test. *$p < 0.05$. (**E**) Freshly isolated human primary NK cells were left untreated (*upper panel*) or treated with PMA (3 h) (*lower panel*), fixed, permeabilized, stained with unlabeled anti-CD16 mAb, followed by DyLight 488–conjugated anti-mouse Ab, and visualized by confocal microscopy. Scale bar, 20 μm. The *right panel* of each figure shows the differential interference contrast image. The images illustrate one representative experiment of three, using cells from independent donors. *$p < 0.05$.

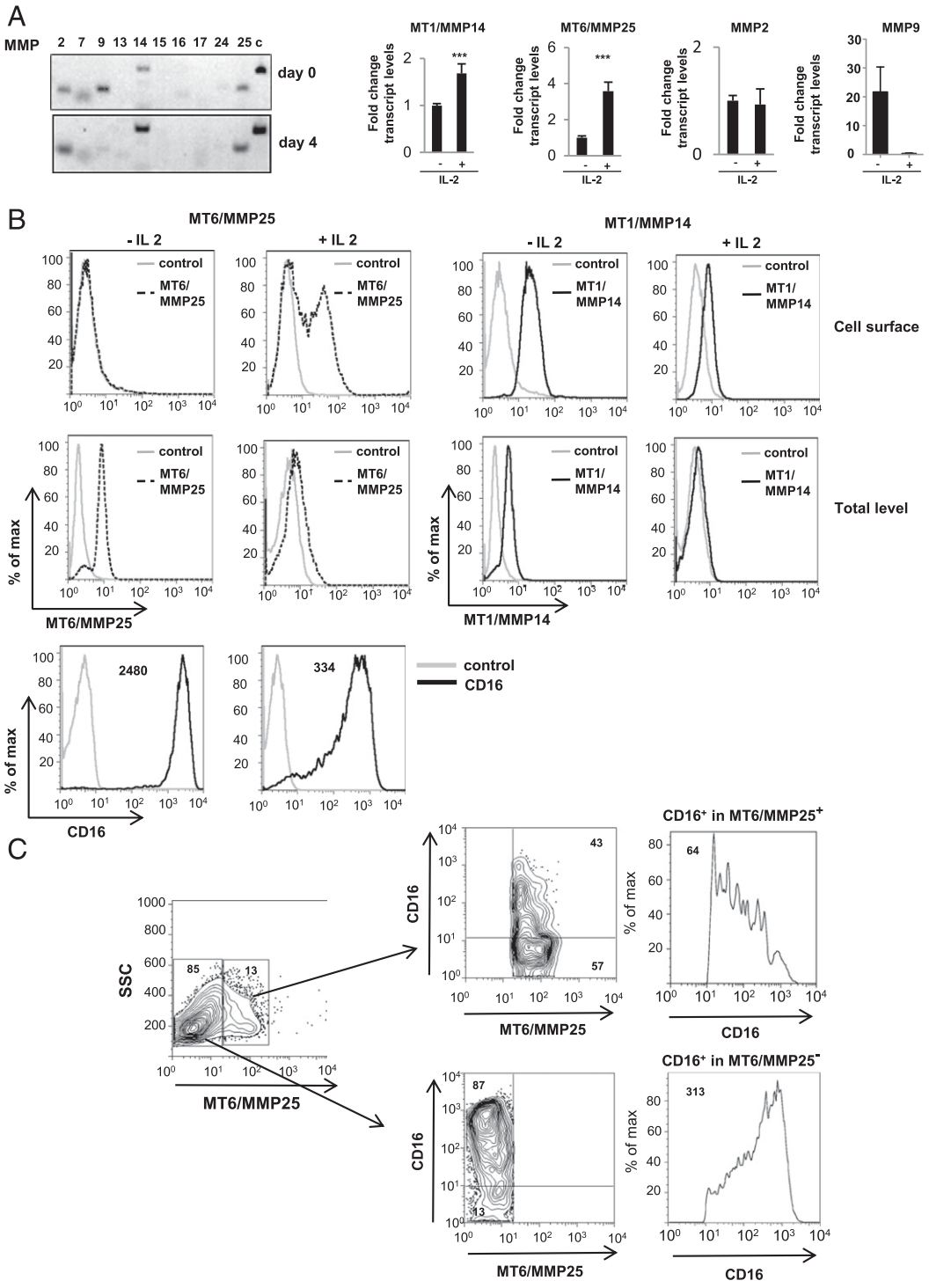


**FIGURE 3.** MT6/MMP25 is expressed by human NK cells and translocates to the cell surface upon IL-2 treatment. (**A**) *Top left panel,* cDNA from freshly isolated human NK cells or NK cells cultured in IL-2 for 4 d was used in RT-PCR with primers for the MMPs listed. *Other panels*, MMP 2, 9, 14 (MT1), and 25 (MT6) transcript levels normalized to 18S rRNA as measured by quantitative PCR. Data are expressed as fold change in transcript levels compared with unstimulated controls, and represent average + SEM from six separate donors. ***$p < 0.001$. (**B**) Freshly isolated or IL-2–activated (day 4, 500 U/ml) human NK cells were analyzed for MT6/MMP25 and MT1/MMP14 expression by flow cytometry. For cell-surface detection, cells were stained with either specific Abs or isotype controls, followed by incubation with FITC-conjugated secondary Ab. In the case of total MMP level staining, cells were permeabilized prior to staining. The *two bottom panels* show CD16 cell-surface expression levels at the same time points. Numbers in the histogram represent MFI values of anti-CD16 staining. Data presented are representative of four independent experiments. (**C**) IL-2–cultured (day 2, 500 U/ml) human NK cells were stained for MT6/MMP25 and CD16 surface expression. The cells divided into MT6/MMP25$^+$ and MT6/MMP25$^-$ subsets were evaluated for their CD16 expression levels. The histograms (*right panels*) show the level of CD16 expression in each subset; the values in the histograms indicate the MFI of CD16. Data presented are representative of three independent experiments.

*panel*), suggesting that the proteinase translocates in a directed manner toward the cell–cell contact site only after NK cell activation. The same result was achieved using a redirected lysis assay, in which NK cells were incubated with P815 target cells (expressing FcRs) in the presence of anti-CD16 mAb. MT6/MMP25 was present at the effector–target interface in the pres-

ence of anti-CD16 Ab (Supplemental Fig. 2). Importantly, the other metalloproteinase upregulated by IL-2, MT1/MMP14, did not polarize or accumulate at the cell–cell contact site upon CD16-mediated synapse formation (Fig. 4B), indicating that MT6/MMP25 accumulation at the CD16-mediated contact site is a specific event caused by NK cell activation.

### *MT6/MMP25 silencing enhances CD16-mediated killing by human primary NK cells*

We have shown that MT6/MMP25 expression correlates with reduced CD16 expression, and it has been reported that CD16 expression levels dictate NK cell ADCC potency; that is, the more receptor expression, the more NK cell effector functions (35, 36). Following this line of reasoning, we hypothesized that if MT6/MMP25 is involved in CD16 downmodulation, then upon disruption of MT6/MMP25 expression with siRNA, we would observe an increase in CD16-mediated ADCC. To verify this hypothesis, we established a cell model using the NK cell line YTS. We stably overexpressed human CD16 and confirmed that this receptor was functional by demonstrating a significant increase in the ADCC capacity of these cells (Supplemental Fig. 3A, 3B). The pattern of expression of MT1/MMP14 and MT6/MMP25 (as well as other tested proteinases) in YTS was similar to that observed in primary NK cells (Supplemental Fig. 3C). An advantage of the YTS NK cell line is that it survives in culture without IL-2, and MT6/MMP25 expression is sequestered intracellularly, as MT6/MMP25 is not detectable on the cell surface (Supplemental Fig. 3D). Using polystyrene beads coated with anti-CD16 mAb, we verified that following the crosslinking of CD16, MT6/MMP25 tends to accumulate at the synapse in YTS cells overexpressing CD16 (cultured without IL-2) (Fig. 5A). Most importantly, the disruption of MT6/MMP25 expression by siRNA in these CD16-transduced YTS cells (Fig. 5B) increased CD16-mediated killing (Fig. 5C), thereby verifying that MT6/MMP25 plays an important role in the function of CD16.

## Discussion

Significant efforts are being devoted to expand NK cells in culture, for therapeutic reinfusion into patients (37–41). In many cases, the key to efficacy of the reinfused NK cells relies on the ability of

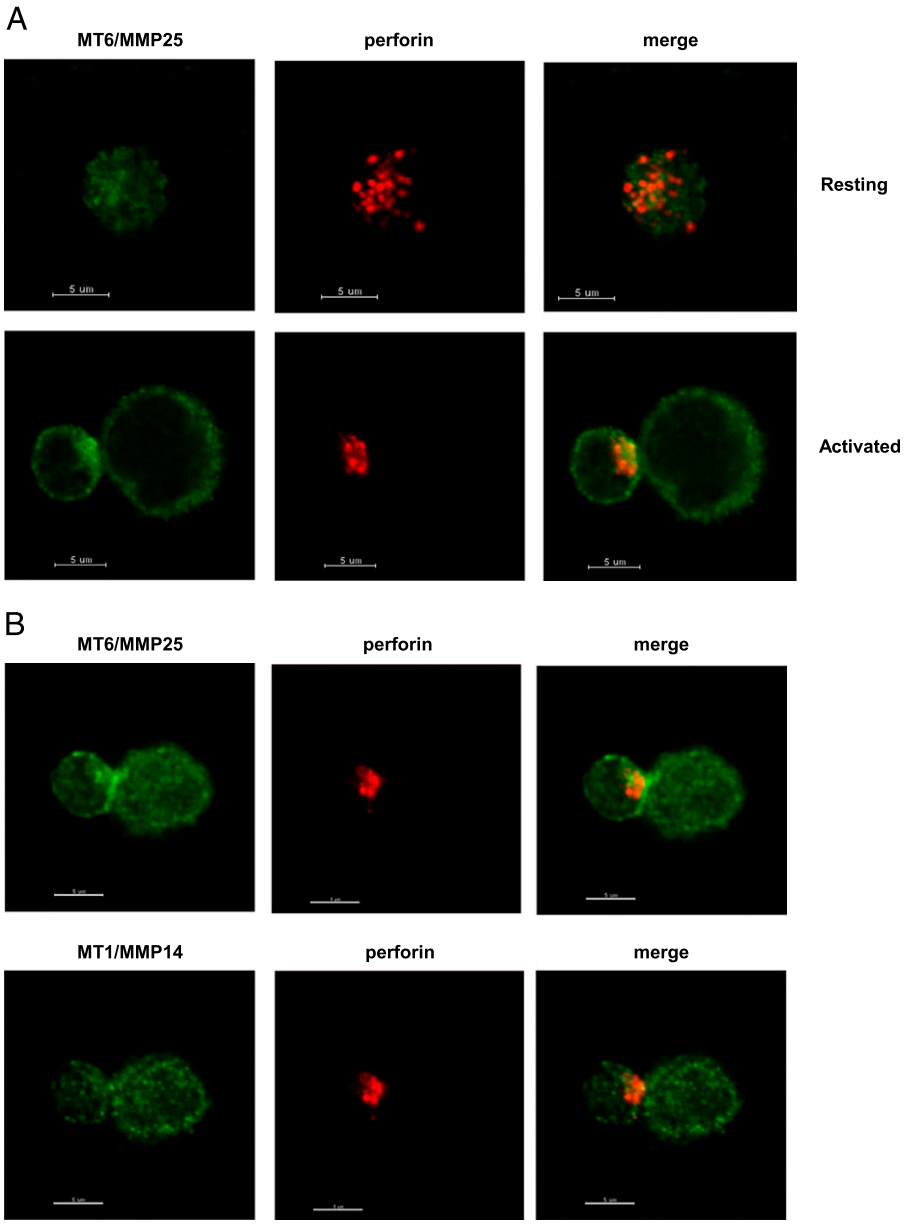


**FIGURE 4.** MT6/MMP25, but not MT1/MMP14, polarizes and accumulates at the contact area between NK cells and target cells. (**A**) Human primary NK cells were left alone (resting; *upper panel*) or were cultured in the presence of IL-2 and mixed with SK-OV3 target cells in the presence of anti-Her2 Ab (activated; *lower panel*). The cells were stained with anti-MT6/MMP25 mAb followed by IgG1-specific DyLight 488–conjugated anti-mouse Ab (green), blocked with 5% normal mouse serum, and then stained with Alexa Fluor 647–conjugated anti-perforin (δG9; red). The distribution of MT6/MMP25 and perforin in the cells was then visualized using confocal microscopy. (**B**) IL-2–activated human primary NK cells conjugated to SK-OV3 target cells in the presence of anti-HER2 Ab were fixed and then stained for perforin, MT6/MMP25, and MT1/MMP14, using specific mAbs. For comparison purposes, MT6/MMP25 and MT1/MMP14 are visualized in green, and the images overlaid with perforin distribution (red) are shown in the *right panels* (merge). Data shown are representative of three independent experiments using different donors. Scale bar in (A) and (B), 5 μm.

CD16 to bind mAbs tailored to the patient's disease, and thereby mediate ADCC. Because a strong positive correlation exists between the level of CD16 expression on NK cells and the potential of NK cells to mediate ADCC (18), investigation of the factors that regulate CD16 cell-surface expression are of clinical relevance. In this study, we investigated the mechanism behind the downregulation of CD16 cell-surface expression in human primary NK cells, owing to activation (PMA induced) and, in particular, exposure to IL-2 (or IL-15) required for NK cell maintenance and expansion in culture.

Our data show that IL-2–induced CD16 downmodulation occurs prior to any measurable proliferation (Fig. 1, Supplemental Fig. 1). Importantly, the downmodulation of CD16 from the cell surface can be reversed by the removal of IL-2 from the culture medium (Fig. 1D) or by the addition of metalloproteinase inhibitors (Fig. 2A), demonstrating that IL-2 is responsible for the induction of CD16 decrease on the cell surface. The downmodulation of CD16 by generalized activation or exposure to IL-2 (or IL-15) appears to be atypical for activating receptors, as primary NK cells dramatically upregulate the expression of other activating receptors, such as NKG2D after cytokine exposure (37, 42). This observation could be related to the fact that unlike other activating receptors CD16 does not require costimulation to elicit a potent signal for cytokine production and release of cytolytic granules, and it also heightens cytokine production owing to costimulation of other receptors (43). Therefore, the end result of CD16 shedding would be the prevention of hyperinflammation leading to autoimmunity. We can only speculate on the fate of the

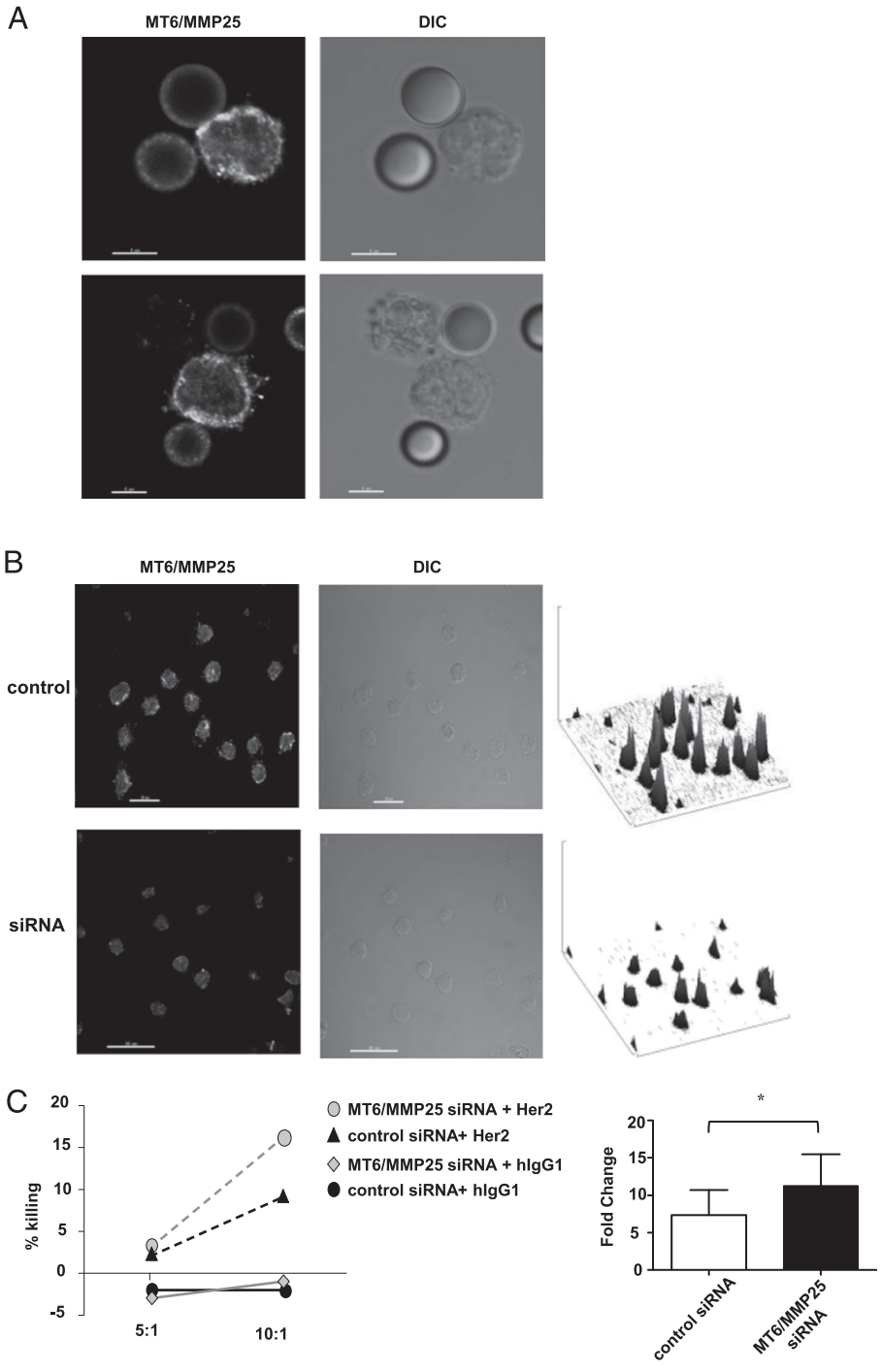


**FIGURE 5.** The CD16-mediated killing by YTS cells is enhanced upon MT6/MMP25 siRNA downmodulation. (**A**) Protein G polystyrene beads (6.8 μm) were precoated with anti-CD16 mAb for 60 min at 4˚C, mixed with YTS/pCDH-CD16 cells, and incubated 45 min at 37˚C; next, they were transferred to slides, fixed, and then stained with anti-MT6/MMP25 mAb, followed by IgG1-specific DyLight 488–conjugated anti-mouse Ab. Two representative images are shown. Scale bar, 5 μm. (**B** and **C**) YTS cells stably transduced with CD16 were nucleofected with 4 μM of MT6/MMP25-specific siRNA duplexes, and 72 h after the nucleofection the CD16-mediated cytotoxicity was measured. (B) MT6/MMP25 protein levels after siRNA downmodulation were evaluated using confocal microscopy. Scale bar, 20 μm. The graphs (*right panel*) show a three-dimensional plot of fluorescence intensity of the confocal images shown (*left panel*). The images shown are representative from ≥ 10 images obtained for each sample analyzed. On the basis of image analysis using ImageJ (see *Materials and Methods*), the silenced samples showed a 2-fold decrease of MT6/MMP25 compared with control samples. (C) SK-OV3 target cells were coated with anti-HER2 mAb (50 ng/ml) or human IgG1 and mixed with YTS/pCDH-CD16 NK cells. The ability of the effector cells to lyse SK-OV3 cells was determined at the indicated E:T ratios (*left panel*). The control sample represents an siRNA universal negative control. The graph (*right panel*) shows the fold change difference in the IgG1/anti-HER2 ratio for control siRNA or MT6/MMP25 siRNA cells. The values were determined from four independent experiments at an E:T ratio of 10:1 and are represented as means + SEM. Statistical analysis was done using the two-tailed paired Student *t* test. $*p < 0.05$.

released CD16 in vivo, and whether it has a biological function. We assume that the amount of CD16 shed into the plasma, which is present at constant levels in healthy individuals, by activated NK cells is small in proportion to the amount shed by neutrophils (44, 45). Soluble CD16 can bind Ab, and it has been shown to have pleiotropic effects on hematopoietic cells (46–48).

Although it is known that CD16 undergoes internalization through endocytosis (49), this was not the case in our study; the treatment of NK cells with endocytosis inhibitors, PAO or dynasore (30, 31), does not restore the activation-induced CD16 downmodulation (Fig. 2C). Moreover, we find that following NK cell activation CD16 does not accumulate inside the cell, and an increased amount of CD16 can be detected in the cell culture supernatant of activated cells (Fig. 2D, 2E). These results demonstrate that CD16 is released from the NK cell surface and support the conclusion that the PMA-induced loss of CD16 is due to shedding and not to endocytosis (Fig. 2D). Indeed, we and others (8, 25) show that the loss of CD16 can be restored by treatment with generic MMP inhibitors (Fig. 2A, 2B), suggesting that this class of proteinases is responsible for the loss of CD16 from activated NK cells.

Our results show that, of the 10 MMPs tested in our study, only MT1/MMP14 and MT6/MMP25 are upregulated by IL-2 in NK cells (Fig. 3). MT1/MMP14 is among the most studied MMPs, as its expression is closely associated with malignant cell invasion (22). MT6/MMP25 is one of the major proteinases produced by polymorphonuclear neutrophils (50), where it is a GPI-anchored MMP mainly localized in secretory granules and partially at the plasma membrane (51). Relocation of active MT6/MMP25 to the plasma membrane in neutrophils occurs upon activation through different stimuli, such as PMA, IL-8, and IL-1α. Our results show that, whereas MT6/MMP25 solely resides intracellularly in freshly isolated NK cells, a significant portion of MT1/MMP14 is present on the cell surface. Of interest, MT6/MMP25 polarizes to the cell–cell contact site following NK cell activation, similarly to perforin (Fig. 4). Our data (Fig. 4A) indicate that MT6/MMP25 is contained in intracellular compartments distinct from lytic granules that, nevertheless, undergo directional secretion in response to NK cell activation. The translocation of MT6/MMP25 from its intracellular sequestration to the cell surface, without the need for new protein synthesis, likely explains the rapidity of CD16 downmodulation (Figs. 3, 4). Our data are thus in agreement with the paradigm that one of the mechanisms for downmodulating activating receptors from the cell surface, besides endocytosis, is cleavage by MMPs (22). In this regard, MT6/MMP25 recruitment to the synapse to possibly downmodulate specific activating molecules makes it a new and important component of NK cell immunological synapse. More experimentation is needed, however, to determine the exact nature of the secretory vesicles in which MT6/MMP25 resides, as well as the precise location of MT6/MMP25 at the CD16-mediated immunological synapse. We are currently investigating the intracellular pathway and mechanism regulating the relocation of MT6/MMP25 to the cell surface upon activation.

The cleavage site motif for a proteinase involves a series of residues that accommodate the proteinase catalytic site, and are labeled as P3-P2-P1-P1′-P2′-P3′, with the cleavage occurring between the P1 and P1′ residues (52). In general, MMPs require hydrophobic amino acids at P1′ and prefer hydrophobic or basic amino acids at P2′ (53). In a recent paper using a proteomic approach (54), the authors identified 286 cleavage sites for MT6/MMP25, with a strong preference for Leu at P1′ and Val at P2′. The juxtamembrane portion of CD16 contains a stretch of small hydrophobic amino acids that could be targeted by metalloproteinases, such as MT6/MMP25. At this point it is not clear, however, whether MT6/MMP25 plays a direct or indirect part in the downmodulation of CD16. MT6/MMP25 has the ability to trigger a proteolytic cascade that activates other MMPs in neutrophils (51). Thus, MT6/MMP25-induced CD16 shedding could be achieved by other MMPs. A recent paper showed that CD16b, the isoform of CD16 expressed in human neutrophils, undergoes shedding by ADAM17 metalloproteinase (55). Nevertheless, our results demonstrate that MT6/MMP25 has an important role in regulating CD16-mediated NK cell activation and effector functions, a conclusion supported by the fact that the disruption of MT6/MMP25 expression enhances NK cell ADCC (Fig. 5).

Although the addition of exogenous MMP inhibitors clearly inhibits the MMP-mediated cleavage of CD16 from the cell surface, it remains an open question regarding whether endogenous MMP inhibitors—in particular, the tissue inhibitors of metalloproteinases (TIMPs)—play a role in protecting the cleavage of cell-surface CD16. All MT-MMPs are sensitive to inhibition by TIMPs (56). Mammalian TIMPs constitute a family of four proteins (TIMP1,-2,-3,-4) that act by binding the catalytic domain of MMPs (57). The individual *TIMP* genes are differentially regulated. TIMP1 and -4 are not expressed in lymphoid tissues (58, 59). Cytokines are known to regulate *TIMPs* expression, but the exact mechanism of this regulation is still ill defined; TGF-β and PMA treatment purportedly downregulates *TIMP-2* and upregulates *TIMP-1* and *TIMP-3* expression in vitro (57). Whether TIMPs are expressed in NK cells and play any role in the IL-2–induced MMP-mediated downmodulation of CD16 will be determined in future studies.

Clearly, cells cultured in IL-2 dramatically downregulate CD16, which correlates with the translocation of MT6 to the cell surface (Fig. 3) and can be alleviated by inhibiting MMPs (Fig. 2). Furthermore, siRNA-mediated knockdown of MT6/MMP25 enhances the capacity of YTS NK cells to mediate ADCC (Fig. 5). Unexpectedly, we could not find a significant difference in the overall expression of CD16 between the cells in which MT6/MMP25 was specifically downmodulated and control treated cells (Supplemental Fig. 4). A likely explanation is that during YTS-mediated ADCC, which does not require activating cytokines in the culture medium, CD16 is cleaved by MT6/MMP25 only at the cell–cell contact site, and taking into consideration the relatively small size of the immunological synapse, one might not be able to detect such small changes in CD16 cell-surface level. This could be particularly true for the primary NK cells that have been cultured in IL-2 prior to the ADCC assay, and thus the bulk of the remaining CD16 (outside the synapse) may reside in membrane locations relatively resistant to MT6 cleavage. Moreover, measuring such small amounts of solubilized CD16 is compounded by the fact that much of it will be associated with target cell debris.

In conclusion, our findings could have important outcomes in clinical settings. Identification of the specific MMP responsible for the shedding of CD16 will allow for the design of specific drugs to prevent cleavage of this potent activating receptor and thus enhance the immunotherapeutic value of NK cells.

## Acknowledgments

We thank the National Institutes of Health Clinical Center Department of Transfusion Medicine for blood samples from healthy human donors collected under protocol 99CC-0168; Joseph Brzostowski, head of the Laboratory of Immunogenetics Imaging Facility (National Institute of Allergy and Infectious Diseases, National Institutes of Health, Rockville, MD), for help and advice for confocal microscopy; and Dr. Wen Jin Wu and Dr. Milos Dokmanovic for the generous gift of Herceptin.

## Disclosures

The authors have no financial conflicts of interest.

## References


1. Vivier, E., D. H. Raulet, A. Moretta, M. A. Caligiuri, L. Zitvogel, L. L. Lanier, W. M. Yokoyama, and S. Ugolini. 2011. Innate or adaptive immunity? The example of natural killer cells. *Science* 331: 44–49.
2. Lanier, L. L. 2005. NK cell recognition. *Annu. Rev. Immunol.* 23: 225–274.
3. Coudert, J. D., J. Zimmer, E. Tomasello, M. Cebecauer, M. Colonna, E. Vivier, and W. Held. 2005. Altered NKG2D function in NK cells induced by chronic exposure to NKG2D ligand-expressing tumor cells. *Blood* 106: 1711–1717.
4. Maxfield, F. R., and T. E. McGraw. 2004. Endocytic recycling. *Nat. Rev. Mol. Cell Biol.* 5: 121–132.
5. Sandusky, M. M., B. Messmer, and C. Watzl. 2006. Regulation of 2B4 (CD244)-mediated NK cell activation by ligand-induced receptor modulation. *Eur. J. Immunol.* 36: 3268–3276.
6. Masilamani, M., G. Peruzzi, F. Borrego, and J. E. Coligan. 2009. Endocytosis and intracellular trafficking of human natural killer cell receptors. *Traffic* 10: 1735–1744.
7. Harrison, D., J. H. Phillips, and L. L. Lanier. 1991. Involvement of a metalloprotease in spontaneous and phorbol ester-induced release of natural killer cell-associated Fc gamma RIII (CD16-II). *J. Immunol.* 147: 3459–3465.
8. Grzywacz, B., N. Kataria, and M. R. Verneris. 2007. CD56(dim)CD16(+) NK cells downregulate CD16 following target cell induced activation of matrix metalloproteinases. Leukemia 21: 356–359; author reply 359.
9. Nimmerjahn, F., and J. V. Ravetch. 2008. Fcgamma receptors as regulators of immune responses. *Nat. Rev. Immunol.* 8: 34–47.
10. Natsume, A., R. Niwa, and M. Satoh. 2009. Improving effector functions of antibodies for cancer treatment: enhancing ADCC and CDC. *Drug Des. Devel. Ther.* 3: 7–16.
11. Shore, S. L., A. J. Nahmias, S. E. Starr, P. A. Wood, and D. E. McFarlin. 1974. Detection of cell-dependent cytotoxic antibody to cells infected with herpes simplex virus. *Nature* 251: 350–352.
12. László, A., I. Petri, and M. Ilyés. 1986. Antibody dependent cellular cytotoxicity (ADCC)-reaction and an in vitro steroid sensitivity test of peripheral lymphocytes in children with malignant haematological and autoimmune diseases. *Acta Paediatr. Acad. Sci. Hung.* 27: 23–29.
13. García-Foncillas, J., and E. Díaz-Rubio. 2010. Progress in metastatic colorectal cancer: growing role of cetuximab to optimize clinical outcome. *Clin. Transl. Oncol.* 12: 533–542.
14. Winter, M. C., and B. W. Hancock. 2009. Ten years of rituximab in NHL. *Expert Opin. Drug Saf.* 8: 223–235.
15. Albertini, M. R., J. A. Hank, and P. M. Sondel. 2005. Native and genetically engineered anti-disialoganglioside monoclonal antibody treatment of melanoma. *Cancer Chemother. Biol. Response Modif.* 22: 789–797.
16. Garnock-Jones, K. P., G. M. Keating, and L. J. Scott. 2010. Trastuzumab: a review of its use as adjuvant treatment in human epidermal growth factor receptor 2 (HER2)-positive early breast cancer. *Drugs* 70: 215–239.
17. Navid, F., V. M. Santana, and R. C. Barfield. 2010. Anti-GD2 antibody therapy for GD2-expressing tumors. *Curr. Cancer Drug Targets* 10: 200–209.
18. Liu, Q., Y. Sun, S. Rihn, A. Nolting, P. N. Tsoukas, S. Jost, K. Cohen, B. Walker, and G. Alter. 2009. Matrix metalloprotease inhibitors restore impaired NK cell-mediated antibody-dependent cellular cytotoxicity in human immunodeficiency virus type 1 infection. *J. Virol.* 83: 8705–8712.
19. Pillet, A. H., F. Bugault, J. Thèze, L. A. Chakrabarti, and T. Rose. 2009. A programmed switch from IL-15- to IL-2-dependent activation in human NK cells. *J. Immunol.* 182: 6267–6277.
20. Caligiuri, M. A., C. Murray, M. J. Robertson, E. Wang, K. Cochran, C. Cameron, P. Schow, M. E. Ross, T. R. Klumpp, R. J. Soiffer, et al. 1993. Selective modulation of human natural killer cells in vivo after prolonged infusion of low dose recombinant interleukin 2. *J. Clin. Invest.* 91: 123–132.
21. Edsparr, K., F. M. Speetjens, A. Mulder-Stapel, R. H. Goldfarb, P. H. Basse, B. Lennernäs, P. J. Kuppen, and P. Albertsson. 2010. Effects of IL-2 on MMP expression in freshly isolated human NK cells and the IL-2-independent NK cell line YT. *J. Immunother.* 33: 475–481.
22. Egeblad, M., and Z. Werb. 2002. New functions for the matrix metalloproteinases in cancer progression. *Nat. Rev. Cancer* 2: 161–174.
23. Somerville, R. P., S. A. Oblander, and S. S. Apte. 2003. Matrix metalloproteinases: old dogs with new tricks. *Genome Biol.* 4: 216.
24. Parks, W. C., C. L. Wilson, and Y. S. López-Boado. 2004. Matrix metalloproteinases as modulators of inflammation and innate immunity. *Nat. Rev. Immunol.* 4: 617–629.
25. Borrego, F., A. Lopez-Beltran, J. Peña, and R. Solana. 1994. Downregulation of Fc gamma receptor IIIA alpha (CD16-II) on natural killer cells induced by anti-CD16 mAb is independent of protein tyrosine kinases and protein kinase C. *Cell. Immunol.* 158: 208–217.
26. Mastroianni, C. M., and G. M. Liuzzi. 2007. Matrix metalloproteinase dysregulation in HIV infection: implications for therapeutic strategies. *Trends Mol. Med.* 13: 449–459.
27. Nagler, A., L. L. Lanier, and J. H. Phillips. 1990. Constitutive expression of high affinity interleukin 2 receptors on human CD16-natural killer cells in vivo. *J. Exp. Med.* 171: 1527–1533.
28. Cacalano, N. A., and J. A. Johnston. 1999. Interleukin-2 signaling and inherited immunodeficiency. *Am. J. Hum. Genet.* 65: 287–293.
29. Procopio, A., A. Gismondi, R. Paolini, S. Morrone, R. Testi, M. Piccoli, L. Frati, R. B. Herberman, and A. Santoni. 1988. Proliferative effects of 12-O-tetradecanoylphorbol-13-acetate (TPA) and calcium ionophores on human large granular lymphocytes (LGL). *Cell. Immunol.* 113: 70–81.
30. Gibson, A. E., R. J. Noel, J. T. Herlihy, and W. F. Ward. 1989. Phenylarsine oxide inhibition of endocytosis: effects on asialofetuin internalization. *Am. J. Physiol.* 257: C182–C184.
31. Ferguson, S. M., and P. De Camilli. 2012. Dynamin, a membrane-remodelling GTPase. *Nat. Rev. Mol. Cell Biol.* 13: 75–88.
32. Edsparr, K., P. H. Basse, R. H. Goldfarb, and P. Albertsson. 2011. Matrix metalloproteinases in cytotoxic lymphocytes impact on tumour infiltration and immunomodulation. *Cancer Microenviron.* 4: 351–360.
33. Kim, M. H., P. Albertsson, Y. Xue, R. P. Kitson, U. Nannmark, and R. H. Goldfarb. 2000. Expression of matrix metalloproteinases and their inhibitors by rat NK cells: inhibition of their expression by genistein. *In Vivo* 14: 557–564.
34. Carter, P., L. Presta, C. M. Gorman, J. B. Ridgway, D. Henner, W. L. Wong, A. M. Rowland, C. Kotts, M. E. Carver, and H. M. Shepard. 1992. Humanization of an anti-p185HER2 antibody for human cancer therapy. *Proc. Natl. Acad. Sci. USA* 89: 4285–4289.
35. Cooper, M. A., T. A. Fehniger, and M. A. Caligiuri. 2001. The biology of human natural killer-cell subsets. *Trends Immunol.* 22: 633–640.
36. Hatjiharissi, E., L. Xu, D. D. Santos, Z. R. Hunter, B. T. Ciccarelli, S. Verselis, M. Modica, Y. Cao, R. J. Manning, X. Leleu, et al. 2007. Increased natural killer cell expression of CD16, augmented binding and ADCC activity to rituximab among individuals expressing the FcgammaRIIIa-158 V/V and V/F polymorphism. *Blood* 110: 2561–2564.
37. Huenecke, S., S. Y. Zimmermann, S. Kloess, R. Esser, A. Brinkmann, L. Tramsen, M. Koenig, S. Erben, C. Seidl, T. Tonn, et al. 2010. IL-2-driven regulation of NK cell receptors with regard to the distribution of CD16+ and CD16- subpopulations and in vivo influence after haploidentical NK cell infusion. *J. Immunother.* 33: 200–210.
38. Miller, J. S., Y. Soignier, A. Panoskaltsis-Mortari, S. A. McNearney, G. H. Yun, S. K. Fautsch, D. McKenna, C. Le, T. E. Defor, L. J. Burns, et al. 2005. Successful adoptive transfer and in vivo expansion of human haploidentical NK cells in patients with cancer. *Blood* 105: 3051–3057.
39. Passweg, J. R., U. Koehl, L. Uharek, S. Meyer-Monard, and A. Tichelli. 2006. Natural-killer-cell-based treatment in haematopoietic stem-cell transplantation. *Best Pract. Res. Clin. Haematol.* 19: 811–824.
40. Koehl, U., J. Sörensen, R. Esser, S. Zimmermann, H. P. Grüttner, T. Tonn, C. Seidl, E. Seifried, T. Klingebiel, and D. Schwabe. 2004. IL-2 activated NK cell immunotherapy of three children after haploidentical stem cell transplantation. *Blood Cells Mol. Dis.* 33: 261–266.
41. Passweg, J. R., M. Stern, U. Koehl, L. Uharek, and A. Tichelli. 2005. Use of natural killer cells in hematopoetic stem cell transplantation. *Bone Marrow Transplant.* 35: 637–643.
42. Park, Y. P., S. C. Choi, P. Kiesler, A. Gil-Krzewska, F. Borrego, J. Weck, K. Krzewski, and J. E. Coligan. 2011. Complex regulation of human NKG2D-DAP10 cell surface expression: opposing roles of the γc cytokines and TGF-β1. *Blood* 118: 3019–3027.
43. Bryceson, Y. T., M. E. March, H.-G. Ljunggren, and E. O. Long. 2006. Synergy among receptors on resting NK cells for the activation of natural cytotoxicity and cytokine secretion. *Blood* 107: 159–166.
44. Huizinga, T. W., M. de Haas, M. Kleijer, J. H. Nuijens, D. Roos, and A. E. von dem Borne. 1990. Soluble Fc gamma receptor III in human plasma originates from release by neutrophils. *J. Clin. Invest.* 86: 416–423.
45. Middelhoven, P. J., J. D. Van Buul, P. L. Hordijk, and D. Roos. 2001. Different proteolytic mechanisms involved in Fc gamma RIIIb shedding from human neutrophils. *Clin. Exp. Immunol.* 125: 169–175.
46. de la Salle, H., J. Galon, H. Bausinger, D. Spehner, A. Bohbot, J. Cohen, J. P. Cazenave, W. H. Fridman, C. Sautès, and D. Hanau. 1997. Soluble CD16/Fc gamma RIII induces maturation of dendritic cells and production of several cytokines including IL-12. *Adv. Exp. Med. Biol.* 417: 345–352.
47. Galon, J., J. F. Gauchat, N. Mazières, R. Spagnoli, W. Storkus, M. Lötze, J. Y. Bonnefoy, W. H. Fridman, and C. Sautès. 1996. Soluble Fcgamma receptor type III (FcgammaRIII, CD16) triggers cell activation through interaction with complement receptors. *J. Immunol.* 157: 1184–1192.
48. Teillaud, C., J. Galon, M. T. Zilber, N. Mazières, R. Spagnoli, R. Kurrle, W. H. Fridman, and C. Sautès. 1993. Soluble CD16 binds peripheral blood mononuclear cells and inhibits pokeweed-mitogen-induced responses. *Blood* 82: 3081–3090.
49. Cecchetti, S., F. Spadaro, L. Lugini, F. Podo, and C. Ramoni. 2007. Functional role of phosphatidylcholine-specific phospholipase C in regulating CD16 membrane expression in natural killer cells. *Eur. J. Immunol.* 37: 2912–2922.
50. Pei, D. 1999. Leukolysin/MMP25/MT6-MMP: a novel matrix metalloproteinase specifically expressed in the leukocyte lineage. *Cell Res.* 9: 291–303.
51. Kang, T., J. Yi, A. Guo, X. Wang, C. M. Overall, W. Jiang, R. Elde, N. Borregaard, and D. Pei. 2001. Subcellular distribution and cytokine- and chemokine-regulated secretion of leukolysin/MT6-MMP/MMP-25 in neutrophils. *J. Biol. Chem.* 276: 21960–21968.
52. Schechter, I., and A. Berger. 1967. On the size of the active site in proteases. I. Papain. *Biochem. Biophys. Res. Commun.* 27: 157–162.
53. Turk, B. E., L. L. Huang, E. T. Piro, and L. C. Cantley. 2001. Determination of protease cleavage site motifs using mixture-based oriented peptide libraries. *Nat. Biotechnol.* 19: 661–667.
54. Starr, A. E., C. L. Bellac, A. Dufour, V. Goebeler, and C. M. Overall. 2012. Biochemical characterization and N-terminomics analysis of leukolysin, the membrane-type 6 matrix metalloprotease (MMP25): chemokine and vimentin cleavages enhance cell migration and macrophage phagocytic activities. *J. Biol. Chem.* 287: 13382–13395.

55. Wang, Y., J. Wu, R. Newton, N. S. Bahaie, C. Long, and B. Walcheck. 2013. ADAM17 cleaves CD16b (FcγRIIIb) in human neutrophils. *Biochim. Biophys. Acta* 1833: 680–685.
56. Sohail, A., Q. Sun, H. Zhao, M. M. Bernardo, J. A. Cho, and R. Fridman. 2008. MT4-(MMP17) and MT6-MMP (MMP25), a unique set of membrane-anchored matrix metalloproteinases: properties and expression in cancer. *Cancer Metastasis Rev.* 27: 289–302.
57. Murphy, G. 2011. Tissue inhibitors of metalloproteinases. *Genome Biol.* 12: 233.
58. Greene, J., M. Wang, Y. E. Liu, L. A. Raymond, C. Rosen, and Y. E. Shi. 1996. Molecular cloning and characterization of human tissue inhibitor of metalloproteinase 4. *J. Biol. Chem.* 271: 30375–30380.
59. Rivera, S., M. Khrestchatisky, L. Kaczmarek, G. A. Rosenberg, and D. M. Jaworski. 2010. Metzincin proteases and their inhibitors: foes or friends in nervous system physiology? *J. Neurosci.* 30: 15337–15357.